

Measurement of the Top Quark Mass

F. Abe,¹⁷ H. Akimoto,³⁹ A. Akopian,³¹ M. G. Albrow,⁷ A. Amadon,⁵ S. R. Amendolia,²⁷ D. Amidei,²⁰ J. Antos,³³ S. Aota,³⁷ G. Apollinari,³¹ T. Arisawa,³⁹ T. Asakawa,³⁷ W. Ashmanskas,¹⁸ M. Atac,⁷ P. Azzi-Bacchetta,²⁵ N. Bacchetta,²⁵ S. Bagdasarov,³¹ M. W. Bailey,²² P. de Barbaro,³⁰ A. Barbaro-Galtieri,¹⁸ V. E. Barnes,²⁹ B. A. Barnett,¹⁵ M. Barone,⁹ G. Bauer,¹⁹ T. Baumann,¹¹ F. Bedeschi,²⁷ S. Behrends,³ S. Belforte,²⁷ G. Bellettini,²⁷ J. Bellinger,⁴⁰ D. Benjamin,³⁵ J. Bensinger,³ A. Beretvas,⁷ J. P. Berge,⁷ J. Berryhill,⁵ S. Bertolucci,⁹ S. Bettelli,²⁷ B. Bevensee,²⁶ A. Bhatti,³¹ K. Biery,⁷ C. Bigongiari,²⁷ M. Binkley,⁷ D. Bisello,²⁵ R. E. Blair,¹ C. Blocker,³ S. Blusk,³⁰ A. Bodek,³⁰ W. Bokhari,²⁶ G. Bolla,²⁹ Y. Bonushkin,⁴ D. Bortoletto,²⁹ J. Boudreau,²⁸ L. Breccia,² C. Bromberg,²¹ N. Bruner,²² R. Brunetti,² E. Buckley-Geer,⁷ H. S. Budd,³⁰ K. Burkett,²⁰ G. Busetto,²⁵ A. Byon-Wagner,⁷ K. L. Byrum,¹ M. Campbell,²⁰ A. Caner,²⁷ W. Carithers,¹⁸ D. Carlsmith,⁴⁰ J. Cassada,³⁰ A. Castro,²⁵ D. Cauz,³⁶ A. Cerri,²⁷ P. S. Chang,³³ P. T. Chang,³³ H. Y. Chao,³³ J. Chapman,²⁰ M.-T. Cheng,³³ M. Chertok,³⁴ G. Chiarelli,²⁷ C. N. Chiou,³³ F. Chlebana,⁷ L. Christofek,¹³ M. L. Chu,³³ S. Cihangir,⁷ A. G. Clark,¹⁰ M. Cobal,²⁷ E. Cocca,²⁷ M. Contreras,⁵ J. Conway,³² J. Cooper,⁷ M. Cordelli,⁹ D. Costanzo,²⁷ C. Couyoumtzelis,¹⁰ D. Cronin-Hennessy,⁶ R. Culbertson,⁵ D. Dagenhart,³⁸ T. Daniels,¹⁹ F. DeJongh,⁷ S. Dell'Agnello,⁹ M. Dell'Orso,²⁷ R. Demina,⁷ L. Demortier,³¹ M. Deninno,² P. F. Derwent,⁷ T. Devlin,³² J. R. Dittmann,⁶ S. Donati,²⁷ J. Done,³⁴ T. Dorigo,²⁵ N. Eddy,²⁰ K. Einsweiler,¹⁸ J. E. Elias,⁷ R. Ely,¹⁸ E. Engels, Jr.,²⁸ W. Erdmann,⁷ D. Errede,¹³ S. Errede,¹³ Q. Fan,³⁰ R. G. Feild,⁴¹ Z. Feng,¹⁵ C. Ferretti,²⁷ I. Fiori,² B. Flaughner,⁷ G. W. Foster,⁷ M. Franklin,¹¹ J. Freeman,⁷ J. Friedman,¹⁹ H. Frisch,⁵ Y. Fukui,¹⁷ S. Gadomski,¹⁴ S. Galeotti,²⁷ M. Gallinaro,²⁶ O. Ganel,³⁵ M. Garcia-Sciveres,¹⁸ A. F. Garfinkel,²⁹ C. Gay,⁴¹ S. Geer,⁷ D. W. Gerdes,¹⁵ P. Giannetti,²⁷ N. Giokaris,³¹ P. Giromini,⁹ G. Giusti,²⁷ M. Gold,²² A. Gordon,¹¹ A. T. Goshaw,⁶ Y. Gotra,²⁵ K. Goulianos,³¹ H. Grassmann,³⁶ L. Groer,³² C. Grosso-Pilcher,⁵ G. Guillian,²⁰ J. Guimaraes da Costa,¹⁵ R. S. Guo,³³ C. Haber,¹⁸ E. Hafen,¹⁹ S. R. Hahn,⁷ R. Hamilton,¹¹ T. Handa,¹² R. Handler,⁴⁰ F. Happacher,⁹ K. Hara,³⁷ A. D. Hardman,²⁹ R. M. Harris,⁷ F. Hartmann,¹⁶ J. Hauser,⁴ E. Hayashi,³⁷ J. Heinrich,²⁶ W. Hao,³⁵ B. Hinrichsen,¹⁴ K. D. Hoffman,²⁹ M. Hohmann,⁵ C. Holck,²⁶ R. Hollebeek,²⁶ L. Holloway,¹³ Z. Huang,²⁰ B. T. Huffman,²⁸ R. Hughes,²³ J. Huston,²¹ J. Huth,¹¹ H. Ikeda,³⁷ M. Incagli,²⁷ J. Incandela,⁷ G. Introzzi,²⁷ J. Iwai,³⁹ Y. Iwata,¹² E. James,²⁰ H. Jensen,⁷ U. Joshi,⁷ E. Kajfasz,²⁵ H. Kambara,¹⁰ T. Kamon,³⁴ T. Kaneko,³⁷ K. Karr,³⁸ H. Kasha,⁴¹ Y. Kato,²⁴ T. A. Keaffaber,²⁵ K. Kelley,¹⁹ R. D. Kennedy,⁷ R. Kephart,⁷ D. Kestenbaum,¹¹ D. Khazins,⁶ T. Kikuchi,³⁷ B. J. Kim,²⁷ H. S. Kim,¹⁴ S. H. Kim,³⁷ Y. K. Kim,¹⁸ L. Kirsch,³ S. Klimenko,⁸ D. Knoblauch,¹⁶ P. Koehn,²³ A. Königeter,¹⁶ K. Kondo,³⁷ J. Konigsberg,⁸ K. Kordas,¹⁴ A. Korytov,⁸ E. Kovacs,¹ W. Kowald,⁶ J. Kroll,²⁶ M. Kruse,³⁰ S. E. Kuhlmann,¹ E. Kuns,³² K. Kurino,¹² T. Kuwabara,³⁷ A. T. Laasanen,²⁹ S. Lami,²⁷ S. Lammel,⁷ J. I. Lamoureux,³ M. Lancaster,¹⁸ M. Lanzoni,²⁷ G. Latino,²⁷ T. LeCompte,¹ S. Leone,²⁷ J. D. Lewis,⁷ P. Limon,⁷ M. Lindgren,⁴ T. M. Liss,¹³ J. B. Liu,³⁰ Y. C. Liu,³³ N. Lockyer,²⁶ O. Long,²⁶ C. Loomis,³² M. Loreti,²⁵ D. Lucchesi,²⁷ P. Lukens,⁷ S. Lusin,⁴⁰ J. Lys,¹⁸ K. Maeshima,⁷ P. Maksimovic,¹⁹ M. Mangano,²⁷ M. Mariotti,²⁵ J. P. Marriner,⁷ A. Martin,⁴¹ J. A. J. Matthews,²² P. Mazzanti,² P. McIntyre,³⁴ P. Melese,³¹ M. Menguzzato,²⁵ A. Menzione,²⁷ E. Meschi,²⁷ S. Metzler,²⁶ C. Miao,²⁰ T. Miao,⁷ G. Michail,¹¹ R. Miller,²¹ H. Minato,³⁷ S. Miscetti,⁹ M. Mishina,¹⁷ S. Miyashita,³⁷ N. Moggi,²⁷ E. Moore,²² Y. Morita,¹⁷ A. Mukherjee,⁷ T. Muller,¹⁶ P. Murat,²⁷ S. Murgia,²¹ H. Nakada,³⁷ I. Nakano,¹² C. Nelson,⁷ D. Neuberger,¹⁶ C. Newman-Holmes,⁷ C.-Y. P. Ngan,¹⁹ L. Nodulman,¹ A. Nomerotski,⁸ S. H. Oh,⁶ T. Ohmoto,¹² T. Ohsugi,¹² R. Oishi,³⁷ M. Okabe,³⁷ T. Okusawa,²⁴ J. Olsen,⁴⁰ C. Pagliarone,²⁷ R. Paoletti,²⁷ V. Papadimitriou,³⁵ S. P. Pappas,⁴¹ N. Parashar,²⁷ A. Parri,⁹ J. Patrick,⁷ G. Pauletta,³⁶ M. Paulini,¹⁸ A. Perazzo,²⁷ L. Pescara,²⁵ M. D. Peters,¹⁸ T. J. Phillips,⁶ G. Piacentino,²⁷ M. Pillai,³⁰ K. T. Pitts,⁷ R. Plunkett,⁷ L. Pondrom,⁴⁰ J. Proudfoot,¹ F. Ptohos,¹¹ G. Punzi,²⁷ K. Ragan,¹⁴ D. Reher,¹⁸ M. Reischl,¹⁶ A. Ribon,²⁵ F. Rimondi,² L. Ristori,²⁷ W. J. Robertson,⁶ T. Rodrigo,²⁷ S. Rolli,³⁸ L. Rosenson,¹⁹ R. Roser,¹³ T. Saab,¹⁴ W. K. Sakumoto,³⁰ D. Saltzberg,⁴ A. Sansoni,⁹ L. Santi,³⁶ H. Sato,³⁷ P. Schlabach,⁷ E. E. Schmidt,⁷ M. P. Schmidt,⁴¹ A. Scott,⁴ A. Scribano,²⁷ S. Segler,⁷ S. Seidel,²² Y. Seiya,³⁷ F. Semeria,² T. Shah,¹⁹ M. D. Shapiro,¹⁸ N. M. Shaw,²⁹ P. F. Shepard,²⁸ T. Shibayama,³⁷ M. Shimojima,³⁷ M. Shochet,⁵ J. Siegrist,¹⁸ A. Sill,³⁵ P. Sinervo,¹⁴ P. Singh,¹³ K. Sliwa,³⁸ C. Smith,¹⁵ F. D. Snider,¹⁵ J. Spalding,⁷ T. Speer,¹⁰ P. Sphicas,¹⁹ F. Spinella,²⁷ M. Spiropulu,¹¹ L. Spiegel,⁷ L. Stanco,²⁵ J. Steele,⁴⁰ A. Stefanini,²⁷ R. Ströhmer,^{7,*} J. Strologas,¹³ F. Strumia,¹⁰ D. Stuart,⁷ K. Sumorok,¹⁹ J. Suzuki,³⁷ T. Suzuki,³⁷ T. Takahashi,²⁴ T. Takano,²⁴ R. Takashima,¹² K. Takikawa,³⁷ M. Tanaka,³⁷ B. Tannenbaum,²² F. Tartarelli,²⁷ W. Taylor,¹⁴ M. Tecchio,²⁰ P. K. Teng,³³ Y. Teramoto,²⁴ K. Terashi,³⁷ S. Tether,¹⁹ D. Theriot,⁷ T. L. Thomas,²² R. Thurman-Keup,¹ M. Timko,³⁸ P. Tipton,³⁰ A. Titov,³¹ S. Tkaczyk,⁷ D. Toback,⁵ K. Tollefson,¹⁹ A. Tollestrup,⁷ H. Toyoda,²⁴

W. Trischuk,¹⁴ J. F. de Troconiz,¹¹ S. Truitt,²⁰ J. Tseng,¹⁹ N. Turini,²⁷ T. Uchida,³⁷ F. Ukegawa,²⁶ J. Valls,³² S. C. van den Brink,²⁸ S. Vejcik III,²⁰ G. Velev,²⁷ R. Vidal,⁷ R. Vilar,^{7,*} D. Vucinic,¹⁹ R. G. Wagner,¹ R. L. Wagner,⁷ J. Wahl,⁵ N. B. Wallace,²⁷ A. M. Walsh,³² C. Wang,⁶ C. H. Wang,³³ M. J. Wang,³³ A. Warburton,¹⁴ T. Watanabe,³⁷ T. Watts,³² R. Webb,³⁴ C. Wei,⁶ H. Wenzel,¹⁶ W. C. Wester III,⁷ A. B. Wicklund,¹ E. Wicklund,⁷ R. Wilkinson,²⁶ H. H. Williams,²⁶ P. Wilson,⁵ B. L. Winer,²³ D. Winn,²⁰ D. Wolinski,²⁰ J. Wolinski,²¹ S. Worm,²² X. Wu,¹⁰ J. Wyss,²⁷ A. Yagil,⁷ W. Yao,¹⁸ K. Yasuoka,³⁷ G. P. Yeh,⁷ P. Yeh,³³ J. Yoh,⁷ C. Yosef,²⁴ T. Yoshida,²⁴ I. Yu,⁷ A. Zanetti,³⁶ F. Zetti,²⁷ and S. Zucchelli²

(CDF Collaboration)

¹Argonne National Laboratory, Argonne, Illinois 60439

²Istituto Nazionale di Fisica Nucleare, University of Bologna, I-40127 Bologna, Italy

³Brandeis University, Waltham, Massachusetts 02254

⁴University of California at Los Angeles, Los Angeles, California 90024

⁵University of Chicago, Chicago, Illinois 60637

⁶Duke University, Durham, North Carolina 27708

⁷Fermi National Accelerator Laboratory, Batavia, Illinois 60510

⁸University of Florida, Gainesville, Florida 32611

⁹Laboratori Nazionali di Frascati, Istituto Nazionale di Fisica Nucleare, I-00044 Frascati, Italy

¹⁰University of Geneva, CH-1211 Geneva 4, Switzerland

¹¹Harvard University, Cambridge, Massachusetts 02138

¹²Hiroshima University, Higashi-Hiroshima 724, Japan

¹³University of Illinois, Urbana, Illinois 61801

¹⁴Institute of Particle Physics, McGill University, Montreal H3A 2T8 and University of Toronto, Toronto M5S 1A7, Canada

¹⁵The Johns Hopkins University, Baltimore, Maryland 21218

¹⁶Institut für Experimentelle Kernphysik, Universität Karlsruhe, 76128 Karlsruhe, Germany

¹⁷National Laboratory for High Energy Physics (KEK), Tsukuba, Ibaraki 305, Japan

¹⁸Ernest Orlando Lawrence Berkeley National Laboratory, Berkeley, California 94720

¹⁹Massachusetts Institute of Technology, Cambridge, Massachusetts 02139

²⁰University of Michigan, Ann Arbor, Michigan 48109

²¹Michigan State University, East Lansing, Michigan 48824

²²University of New Mexico, Albuquerque, New Mexico 87131

²³The Ohio State University, Columbus, Ohio 43210

²⁴Osaka City University, Osaka 588, Japan

²⁵Università di Padova, Istituto Nazionale di Fisica Nucleare, Sezione di Padova, I-35131 Padova, Italy

²⁶University of Pennsylvania, Philadelphia, Pennsylvania 19104

²⁷Istituto Nazionale di Fisica Nucleare, University and Scuola Normale Superiore of Pisa, I-56100 Pisa, Italy

²⁸University of Pittsburgh, Pittsburgh, Pennsylvania 15260

²⁹Purdue University, West Lafayette, Indiana 47907

³⁰University of Rochester, Rochester, New York 14627

³¹Rockefeller University, New York, New York 10021

³²Rutgers University, Piscataway, New Jersey 08855

³³Academia Sinica, Taipei, Taiwan 11530, Republic of China

³⁴Texas A&M University, College Station, Texas 77843

³⁵Texas Tech University, Lubbock, Texas 79409

³⁶Istituto Nazionale di Fisica Nucleare, University of Trieste/Udine, Italy

³⁷University of Tsukuba, Tsukuba, Ibaraki 315, Japan

³⁸Tufts University, Medford, Massachusetts 02155

³⁹Waseda University, Tokyo 169, Japan

⁴⁰University of Wisconsin, Madison, Wisconsin 53706

⁴¹Yale University, New Haven, Connecticut 06520

(Received 30 September 1997)

We present a measurement of the top quark mass using a sample of $t\bar{t}$ decays into an electron or a muon, a neutrino, and four jets. The data were collected in $p\bar{p}$ collisions at $\sqrt{s} = 1.8$ TeV with the Collider Detector at Fermilab and correspond to an integrated luminosity of 109 pb^{-1} . We measure the top quark mass to be $175.9 \pm 4.8(\text{stat}) \pm 4.9(\text{syst}) \text{ GeV}/c^2$. [S0031-9007(98)05578-1]

PACS numbers: 14.65.Ha, 13.85.Ni, 13.85.Qk

The top quark mass is a fundamental parameter of the standard model and is needed for extracting other parameters from precision electroweak measurements.

The first direct measurement of its value was made by CDF [1] and was based on 19 pb^{-1} of data. Updated measurements were reported by both the CDF and D0

Collaborations using significantly more data [2–6]. In this paper we present a new measurement of the top quark mass with greatly improved precision, using our entire data sample from the 1992–1995 runs, which corresponds to a total integrated luminosity of $109 \pm 7 \text{ pb}^{-1}$ [7]. This new measurement supersedes the results reported in [1,2].

Within the standard model, the top quark decays more than 99% of the time into Wb . The W boson can then decay to a quark-antiquark or lepton-neutrino pair. The measurement presented here uses events with a $t\bar{t}$ pair decaying in the “lepton + jets” channel. This channel is characterized by a single high- P_T [1] lepton (electron or muon) and missing transverse energy from a $W \rightarrow \ell\nu$ decay, plus several jets coming from a hadronically decaying W boson and from the b quarks from the top quark decays. Jets formed by the fragmentation of b quarks can be identified (“tagged”) either by reconstructing secondary vertices from b hadron decays with the silicon vertex detector (SVX tagging), or by finding additional leptons from semileptonic b decays (SLT tagging). The SVX and SLT tagging algorithms are described in Ref. [2].

To be used for the mass measurement, events must contain a single isolated electron (muon) with E_T (P_T) $> 20 \text{ GeV}$ (GeV/c) in the central region of the detector ($|\eta| < 1$) and missing transverse energy, $\cancel{E}_T \geq 20 \text{ GeV}$, indicating the presence of a neutrino. At least four jets are required in each event, three of which must have an observed $E_T \geq 15 \text{ GeV}$ and $|\eta| \leq 2$. In order to increase the acceptance, we relax the requirements on the fourth jet to be $E_T \geq 8 \text{ GeV}$ and $|\eta| \leq 2.4$, provided one of the four leading jets is tagged by the SVX or SLT algorithms. SVX tags are allowed only on jets with observed $E_T \geq 15 \text{ GeV}$, while SLT tags are allowed on jets with $E_T \geq 8 \text{ GeV}$. If no such tag is present, the fourth jet must satisfy the same E_T and η requirements as the first three. All jets in this analysis are formed as clusters of calorimeter towers within cones of fixed radius $\Delta R \equiv \sqrt{\Delta\eta^2 + \Delta\phi^2} = 0.4$ [8]. The above selection defines our mass sample, which contains 83 events.

Measurement of the top quark mass begins by fitting each event in the sample to the hypothesis of $t\bar{t}$ production followed by decay in the lepton + jets channel,

$$p\bar{p} \rightarrow t\bar{t} + X,$$

$$t \rightarrow W^+ b \rightarrow \ell^+ \nu b \quad \text{or} \quad q\bar{q}' b,$$

$$\bar{t} \rightarrow W^- \bar{b} \rightarrow q\bar{q}' \bar{b} \quad \text{or} \quad \ell^- \bar{\nu} \bar{b}.$$

The three-momenta of the lepton and the b , \bar{b} , q , and \bar{q}' quarks are measured from the observed lepton and four leading jets in the event; the mass of the b is set to $5 \text{ GeV}/c^2$, that of q and \bar{q}' to $0.5 \text{ GeV}/c^2$. The neutrino mass is assumed to be zero and its momentum is not measured, thereby yielding three unknowns. The two transverse momentum components of X are measured from the extra jets in the event and the energy that is detected but not collected in jet or electron clusters. Five constraints are applied: The transverse momentum components of the entire $t\bar{t} + X$ system must be zero,

the invariant masses of the lepton-neutrino and $q\bar{q}'$ pairs must each equal the W boson mass, and the mass of the top quark must equal that of the antitop quark. The problem, therefore, has two extra constraints and is solved by a standard χ^2 -minimization technique. The output of each event fit is a reconstructed top mass M_{rec} and a χ^2 value quantifying how well the event is described by the $t\bar{t}$ hypothesis.

Electron energies and muon momenta entering the fit are measured with the calorimeter and tracking chambers, respectively [9]. Jet energies are corrected for losses in cracks between detector components, absolute energy scale, contributions from the underlying event and multiple interactions, and losses outside the clustering cone. These corrections are determined from a combination of Monte Carlo simulations and data [10]. The four leading jets in a $t\bar{t}$ candidate event undergo an additional energy correction that depends on the type of parton they are assigned to in the fit: a light quark, a hadronically decaying b quark, or a b quark that decayed semileptonically [1]. This parton-specific correction was derived from a study of $t\bar{t}$ events generated with the HERWIG Monte Carlo program [11,12].

There are twelve distinct ways of assigning the four leading jets to the four partons b , \bar{b} , q , and \bar{q}' . In addition, there is a quadratic ambiguity in the determination of the longitudinal component of the neutrino momentum. This yields up to 24 different configurations for reconstructing an event according to the $t\bar{t}$ hypothesis. We require that SVX or SLT-tagged jets be assigned to b partons and choose the configuration with lowest χ^2 . Events with $\chi^2 > 10$ are rejected. In the mass sample, 76 out of 83 events remain after this cut. When all parton-jet assignments are correctly made, the resolution of the reconstructed mass is $13 \text{ GeV}/c^2$ for a top mass of $175 \text{ GeV}/c^2$.

A maximum-likelihood method is used to extract a top mass measurement from a sample of events which have been reconstructed according to the $t\bar{t}$ hypothesis. An essential ingredient of the likelihood function is the probability density $f_s(M_{\text{rec}} | M_{\text{top}})$ to reconstruct a mass M_{rec} from a $t\bar{t}$ event if the true top mass is M_{top} . In past publications [1,2] we estimated f_s for a discrete set of M_{top} values by smoothing histograms of M_{rec} for events from a HERWIG Monte Carlo calculation. In the present analysis we parametrize f_s as a smooth function of both M_{rec} and M_{top} [13]. This new approach yields a consistent, M_{top} -dependent way of dealing with low statistics in the tails of the M_{rec} histograms and produces a continuous likelihood shape from which the top mass and its uncertainty can be extracted. The probability density $f_b(M_{\text{rec}})$ for reconstructing a mass M_{rec} from a background event is obtained by fitting a smooth function to a mass distribution generated with the VECBOS [14] $W + \text{jets}$ Monte Carlo program.

The likelihood function is the product of three factors:

$$\mathcal{L} = \mathcal{L}_{\text{shape}} \times \mathcal{L}_{\text{backgr}} \times \mathcal{L}_{\text{param}}, \quad (1)$$

where $\mathcal{L}_{\text{shape}}$ represents the joint probability density for a sample of N reconstructed masses M_i to be drawn from a population with a background fraction x_b :

$$\mathcal{L}_{\text{shape}} = \prod_{i=1}^N [(1 - x_b)f_s(M_i | M_{\text{top}}) + x_b f_b(M_i)].$$

The fraction x_b is constrained by an independent measurement that is summarized by the background likelihood $\mathcal{L}_{\text{backgr}}$. The function $\mathcal{L}_{\text{param}}$ allows the parametrizations of f_s and f_b to vary within the uncertainties returned by the fits to the HERWIG and VECBOS histograms of M_{rec} . By including $\mathcal{L}_{\text{param}}$ in the likelihood definition, the uncertainty due to the finite statistics of these histograms is incorporated into the statistical uncertainty on the measured top mass. The likelihood \mathcal{L} is maximized with respect to M_{top} , x_b , and the parameters that define the shapes of f_s and f_b .

The precision of the top quark mass measurement is expected to increase with the number of observed events, the signal-over-background ratio, and the narrowness of the reconstructed-mass distribution. These characteristics vary significantly between samples with different b tagging requirements. Therefore, to make optimal use of all of the available information, we partition the mass sample into nonoverlapping subsamples, define subsample likelihoods according to Eq. (1), and maximize the product of these likelihoods to determine the top mass and its uncertainty [15]. The use of nonoverlapping subsamples ensures that the corresponding likelihoods are statistically uncorrelated. Monte Carlo studies show that an optimum partition is made up of four subsamples: events with a single SVX tag, events with two SVX tags, events with an SLT tag but no SVX tag, and events with no tag but with the tighter kinematic requirement of four jets with $E_T \geq 15$ GeV and $|\eta| \leq 2$.

The calculation of the expected background content of each subsample starts from the background calculation performed on the $W + \geq 3$ -jet sample for the $t\bar{t}$ cross section measurement [7]. The extrapolation to the mass subsamples takes into account the additional requirement of a fourth jet, the χ^2 cut on event reconstruction, and the fact that SVX and SLT tags are counted only if they are on one of the four leading jets. The efficiencies of these requirements are determined from Monte Carlo studies. They are used together with background rates and tagging efficiencies from the cross section analysis to predict the total number of events in each mass subsample as a function of the unknown numbers of $t\bar{t}$ and $W + \text{jet}$ events in the combined sample. These unknowns are estimated by maximizing a multinomial likelihood that constrains the predicted subsample sizes to the observed ones. This procedure generates the expected background fractions shown in Table I and the background likelihood $\mathcal{L}_{\text{backgr}}$ used in Eq. (1).

Approximately 67% of the background in the entire mass sample comes from $W + \text{jet}$ events. Another 20% consists of multijet events where a jet is misidentified

as a lepton and $b\bar{b}$ events with a b hadron decaying semileptonically. The remaining 13% is made up of $Z + \text{jet}$ events where the Z -boson decays leptonically, events with a WW , WZ , or ZZ diboson, and single-top production. We have compared the reconstructed-mass distributions in VECBOS and data for three event selections that are expected to be depleted in $t\bar{t}$ events [16]. These selections are slight variations of the mass sample selection. The first one requires that the primary lepton be an electron with a pseudorapidity in the range $1.1 \leq |\eta| \leq 2.4$ instead of $|\eta| \leq 1$, and yields 26 data events. The second one requires at least four jets with $E_T \geq 8$ GeV and $|\eta| \leq 2.4$, but no more than two jets with $E_T \geq 15$ GeV and $|\eta| \leq 2$. This results in 243 data events. The third selection requires events with a nonisolated primary lepton and yields 164 data events. In all three cases, a Kolmogorov-Smirnov test applied to the comparison of VECBOS and data yields a confidence level of at least 30%. We, therefore, use the VECBOS calculation to determine the shape of f_b for the likelihood function.

The reconstructed-mass distribution of the sum of the four subsamples is plotted in Fig. 1. The inset shows the shape of the corresponding sum of negative log-likelihoods as a function of top mass. From this we measure $M_{\text{top}} = 175.9 \pm 4.8$ GeV/ c^2 , where the uncertainty corresponds to a half-unit change in the negative log-likelihood with respect to its minimum. Monte Carlo studies on mass samples similar to ours yield an 11% probability for obtaining a statistical uncertainty of this size or smaller. The background fractions x_b returned by the fit agree with the x_b^0 numbers listed in Table I. To judge the goodness of the fit of the combined M_{rec} distribution, we performed a Kolmogorov-Smirnov test and obtained a confidence level of 64%. The reconstructed-mass distribution in each of the four subsamples is compared to the result of the combined fit in Fig. 2. The insets show the results of likelihood fits performed separately in each of the four subsamples. The mass measurements obtained from these fits are consistent with each other, as shown in Table I.

We list the systematic uncertainties in Table II. The largest one comes from the jet energy measurement. Each of the jet energy corrections described earlier carries with it a separate, energy-dependent uncertainty [10]. Recent

TABLE I. Subsamples of $W + \geq 4$ -jet events that are used for the top quark mass measurement. For each subsample, the number of observed events N_{obs} , the expected background fraction x_b^0 , and the measured top mass M_{top} are shown. Uncertainties on the measured top mass are statistical only.

Subsample	N_{obs}	x_b^0 (%)	Measured M_{top} (GeV/ c^2)
SVX double tag	5	5 ± 3	170.1 ± 9.3
SVX single tag	15	13 ± 5	178.0 ± 7.9
SLT tag (no SVX)	14	40 ± 9	142_{-14}^{+33}
No tag ($E_T(j_4) \geq 15$ GeV)	42	56 ± 15	181.0 ± 9.0

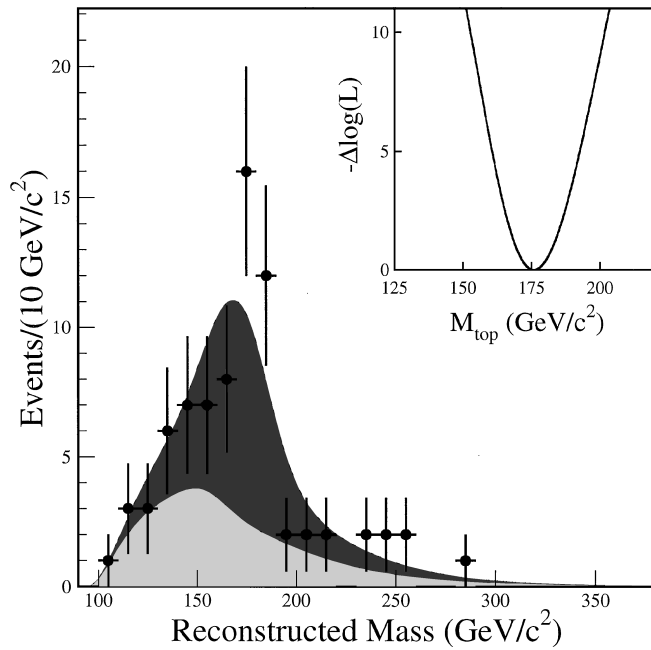


FIG. 1. Reconstructed-mass distribution of the four mass subsamples combined. The data (points) are compared with the result of the combined fit (dark shading) and with the background component of the fit (light shading). The inset shows the variation of the combined negative log-likelihood with M_{top} .

studies of soft gluon radiation outside the jet clustering cone have reduced the uncertainty from this source to 2.5% for a jet with observed $E_T > 40$ GeV. For an observed jet E_T of 40 GeV, the total uncertainty on the corrected E_T varies between 3.4% and 5.6% depending on the proximity of the jet to cracks between detector components. We have checked the jet correction procedure and the evaluation of the jet energy scale uncertainty with events containing a leptonically decaying Z boson and one jet. A study of how the transverse momentum of the jet balances that of the Z decay products finds that the observed ratio of $[P_T(Z) - P_T(\text{jet})]/P_T(Z)$ differs by $[3.2 \pm 1.5(\text{stat}) \pm 4.1(\text{syst})]\%$ from Monte Carlo simulations. The 4.1% systematic uncertainty is due to the jet energy scale only. Since the difference is consistent with zero, this study independently confirms the soundness of our estimate of the jet energy scale uncertainty. A further confirmation was obtained by measuring the mass of the W boson from its hadronic decay modes, using a sample of $t\bar{t}$ candidate events in the lepton + jets channel. This measurement yields $77.2 \pm 3.5(\text{stat}) \pm 2.9(\text{syst}) \text{ GeV}/c^2$ [17].

The second largest systematic uncertainty is due to high transverse momentum gluons that are radiated from the initial or final state of a $t\bar{t}$ event and sometimes take the place of a $t\bar{t}$ decay product among the four leading jets. This uncertainty was determined with the PYTHIA Monte Carlo calculation [18] by separately studying the effect of extra jets coming from initial and final state radiation.

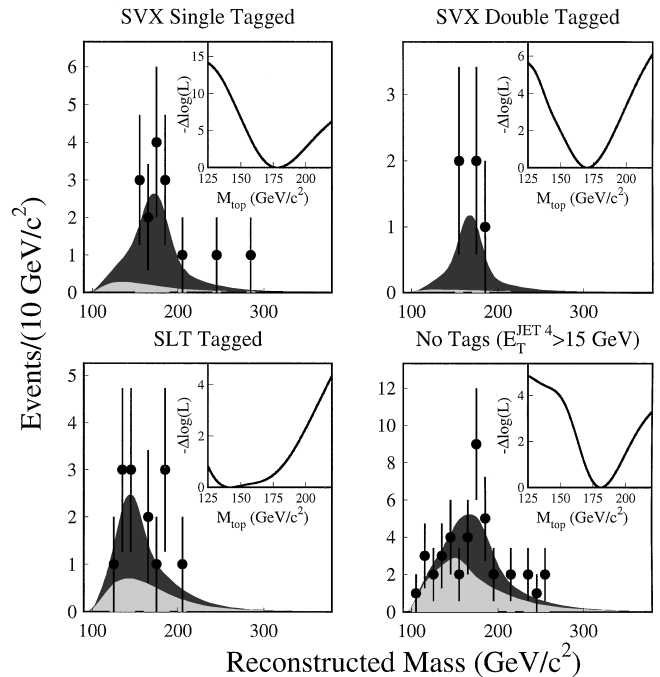


FIG. 2. Reconstructed-mass distributions in each of the four mass subsamples. Each plot shows the data (points), the result of the combined fit to top + background (dark shading), and the background component of the fit (light shading). The insets show the variation of the negative log-likelihoods with M_{top} for the separate subsample fits.

The uncertainty in the modeling of the background mass distribution was estimated by varying the Q^2 scale in VECBOS. Additional sources of uncertainty include the kinematical bias introduced by b tagging and the choice of parton distribution functions (CTEQ4L [19] vs MRSD0'). The sum in quadrature of all the systematic uncertainties is $4.9 \text{ GeV}/c^2$. We have investigated the effect of using Monte Carlo calculations other than HERWIG to model $t\bar{t}$ events. Whereas PYTHIA yields the same measured mass, ISAJET [20] leads to a $+1.5 \text{ GeV}/c^2$ shift. We do not include this as a separate uncertainty since the main difference between these calculations, namely the modeling of gluon radiation and jet fragmentation, is already accounted for in our analysis of other systematic uncertainties.

In summary, we have measured the top quark mass to be $175.9 \pm 4.8(\text{stat}) \pm 4.9(\text{syst}) \text{ GeV}/c^2$. This is the most precise determination of the top mass to date. A

TABLE II. List of systematic uncertainties on the final top quark mass measurement.

Source	Value (GeV/c^2)
Jet energy measurement	4.4
Initial and final state radiation	1.8
Shape of background spectrum	1.3
b tag bias	0.4
Parton distribution functions	0.3
Total	4.9

new technique for optimizing the use of the information provided by the tagging algorithms has resulted in a smaller statistical uncertainty, and a better understanding of the jet energy scale has led to a reduced systematic uncertainty. In addition, the probability densities for reconstructed masses are now fully parametrized, which simplifies the likelihood analysis and the treatment of the finite statistics of the Monte Carlo event samples.

We thank the Fermilab staff and the technical staffs of the participating institutions for their vital contributions. This work is supported by the U.S. Department of Energy and the National Science Foundation, the Natural Sciences and Engineering Research Council of Canada, the Istituto Nazionale di Fisica Nucleare of Italy, the Ministry of Education, Science and Culture of Japan, the National Science Council of the Republic of China, and the A. P. Sloan Foundation.

*Visitor.

- [1] F. Abe *et al.*, Phys. Rev. D **50**, 2966 (1994); F. Abe *et al.*, Phys. Rev. Lett. **73**, 225 (1994). A description of the CDF detector can be found in: F. Abe *et al.*, Nucl. Instrum. Methods Phys. Res., Sect. A **271**, 387 (1988), and references therein; D. Amidei *et al.*, *ibid.* **350**, 73 (1994); P. Azzi *et al.*, *ibid.* **360**, 137 (1995).
- [2] F. Abe *et al.*, Phys. Rev. Lett. **74**, 2626 (1995).
- [3] S. Abachi *et al.*, Phys. Rev. Lett. **74**, 2632 (1995).
- [4] S. Abachi *et al.*, Phys. Rev. Lett. **79**, 1197 (1997).
- [5] F. Abe *et al.*, Phys. Rev. Lett. **79**, 1992 (1997).
- [6] F. Abe *et al.*, this issue, Phys. Rev. Lett. **80**, 2779 (1998).
- [7] F. Abe *et al.*, following Letter, Phys. Rev. Lett. **80**, 2773 (1998).
- [8] F. Abe *et al.*, Phys. Rev. D **45**, 1448 (1992).
- [9] F. Abe *et al.*, Phys. Rev. D **52**, 4784 (1995).
- [10] F. Abe *et al.*, Phys. Rev. D **47**, 4857 (1993).
- [11] G. Marchesini and B. R. Webber, Nucl. Phys. **B310**, 461 (1988); G. Marchesini *et al.*, Comput. Phys. Commun. **67**, 465 (1992). We use HERWIG version 5.6.
- [12] The default set of structure functions in all our Monte Carlo calculations is MRSD0' [A. D. Martin, R. G. Roberts, and W. J. Stirling, Phys. Lett. B **306**, 145 (1993)].
- [13] S. Bettelli, Laurea thesis, University of Pisa, 1996.
- [14] F. A. Berends, W. T. Giele, H. Kuijf, and B. Tausk, Nucl. Phys. **B357**, 32 (1991).
- [15] K. Tollefson, Ph.D. thesis, University of Rochester, 1997.
- [16] N. Eddy, Ph.D. thesis, University of Michigan, 1997.
- [17] F. Abe *et al.*, Report No. Fermilab-Pub-97/285-E (to be published).
- [18] T. Sjöstrand, Comput. Phys. Commun. **82**, 74 (1994). We use PYTHIA version 5.7.
- [19] H. L. Lai *et al.*, Phys. Rev. D **55**, 1280 (1997).
- [20] F. Paige and S. Protopopescu, BNL Report No. 38034, 1986 (unpublished). We use ISAJET version 7.06.